NanoImpact 12 (2018) 42–50

Contents lists available at ScienceDirect

NanoImpact

journal homepage: www.elsevier.com/locate/nanoimpact

# Reduced expression of iron transport and homeostasis genes in *Pseudomonas fluorescens* during iron uptake from nanoscale iron☆

Sanjivni Sinha[a], Tonoy K. Das[a], Achintya N. Bezbaruah[a,*,1], Ann-Marie Fortuna[b,c,**,1]

[a] Nanoenvirology Research Group, Civil and Environmental Engineering, North Dakota State University, United States of America
[b] Grazinglands Research Laboratory, USDA-ARS, El Reno, OK, United States of America
[c] Department of Soil Science, North Dakota State University, United States of America

ARTICLE INFO

*Keywords:*
Bacterioferritin-associated ferredoxin
EDS
Iron acquisition
NZVI
*P. fluorescens*
Pyoverdine biosynthesis gene *pvdS*
qRT-PCR
Siderophore production
TEM

ABSTRACT

Plant growth-promoting rhizobacteria (PGPR) have beneficial effects on the host plant that include acquisition of nutrients such as iron (Fe). In this study, the impact of varying concentrations of nanoscale zero-valent iron (NZVI, 1, 2 and 5 g $L^{-1}$) on a PGPR, *Pseudomonas fluorescens*' viability, growth and production of siderophores was investigated. Microscale zero-valent iron (MZVI) particles were also included in this study to determine and compare the effects of particle size on Fe acquisition and use by *Pseudomonas fluorescens*. Siderophores chelate insoluble forms of Fe that are then rendered bioavailable to *P. fluorescens* as well as some plants. This research indicates that the Fe species derived from lower concentrations of NZVI additions (1 g $L^{-1}$) are bioavailable and can be utilized as a nutrient by *P. fluorescens* without the bacteria producing siderophores, an energy intensive process. Also, NZVI application as a fertilizer has promise for better utilization of Fe by plants. *P. fluorescens* colony forming units (log10 CFU $mL^{-1}$) growth in cultures containing 1 g $L^{-1}$ NZVI were significantly higher exceeded (14 units) than those grown without NZVI additions (13 units). The majority of *P. fluorescens* cells treated with 2 and 5 g $L^{-1}$ were nonviable and produced limited colony forming units (4 units). The effects of NZVI on siderophore production by *P. fluorescens* were assessed using chrome azurol S (CAS) plates and real time quantitative reverse transcription PCR (qRT-PCR). Further, expression of genes involved in Fe utilization [putative pvdS (PFL 4190) and a bacterioferritin-associated ferredoxin gene (PFL 4858)] were targeted using real time quantitative reverse transcription PCR (qRT-PCR). Expression of both genes was below detection limits in cultures exposed to NZVI but measurable in MZVI and control treatments, again indicating potential ease in uptake of Fe by *P. fluorescens* from NZVI. Transmission electron microscopy (TEM) revealed the presence of NZVI particles on the exterior and interior of cells; energy dispersive X-ray spectroscopy (EDS) verified that the material was derived from NZVI and that Fe concentrations were higher in the interior of cells exposed to 1 g $L^{-1}$ NZVI compared to the control. The research findings from this study indicate that NZVI has the potential to accumulate in plant growth-promoting rhizobacteria and affect the growth of organisms in environments like the rhizobiome which may affect plant growth positively. This research opens up opportunities for future studies to determine the effects of Fe and other nutrients and micronutrients derived from nanomaterials, particularly in oligotrophic systems.

## 1. Introduction

Nanotechnology has been widely accepted in various sectors including biomedical, personal care, industrial, electronics, food packaging, electronics, agricultural products (pesticides and insecticides) and environmental remediation. Iron-based nanomaterial, specifically nanoscale zero-valent iron (NZVI), is one of the most frequently used nanoparticles that has shown promise for environmental

*Abbreviations:* CAS, chrome azurol S; CFU, colony forming units; NZVI, nanoscale zero-valent iron; ORP, in oxidation reduction potential; PGPR, plant growth promoting rhizobacteria; *P. fluorescens*, *Pseudomonas fluorescens*; *pvdS*, pyoverdine synthesis gene; EDS, energy dispersive X-ray spectroscopy; ROS, reactive oxygen species; TEM, transmission electron microscopy

☆ Notes: the authors declare no competing financial interest.

* Corresponding author.
** Corresponding author at: Department of Soil Science, North Dakota State University, United States of America.
*E-mail addresses:* a.bezbaruah@ndsu.edu (A.N. Bezbaruah), Ann-Marie.Fortuna@ars.usda.gov (A.-M. Fortuna).

[1] Both corresponding authors have contributed equally.

https://doi.org/10.1016/j.impact.2018.08.009
Received 17 April 2018; Received in revised form 31 July 2018; Accepted 30 August 2018
Available online 06 September 2018

remediation (Almeelbi and Bezbaruah 2012; Krajangpan et al. 2012; Stefaniuk et al. 2016; Tosco et al. 2014). Almeelbi and Bezbaruah (Almeelbi and Bezbaruah 2014) demonstrated the possible use of NZVI as a fertilizer for plants and reported significantly higher iron content in spinach (*Spinacia oleracea* L.) grown hydroponically with NZVI as a nutrient additive. There has been increased interest in aqueous phosphate removal using NZVI (Almeelbi and Bezbaruah 2012; Sleiman et al. 2016, 2017; D. Wu et al. 2013a; D.L. Wu et al. 2013b). Despite the benefits of using NZVI for remediation and as a plant nutrient, there are reports of microorganisms being adversely affected by Fe-nanoparticles (Kumar et al. 2014b; Lefevre et al. 2016; Ludovica Sacca et al. 2014; D.L. Wu et al. 2013b; Yang et al. 2013). Biological processes that control nutrient cycling may be negatively impacted at concentrations of NZVI as low as 0.2 mg $mL^{-1}$ (D.L. Wu et al. 2013b) while doses recommended for environmental remediation often range between 1 and 10 mg $mL^{-1}$ (i.e., 1–10 g $L^{-1}$) (Bruton et al. 2015).

Therefore, a more complete understanding of the mechanisms controlling bacterial inhibition and growth resulting from exposure to NZVI is needed. Iron is a micronutrient required for biological functions and a co-factor of many enzymatic reactions in bacteria (Aitken et al. 2006). However, high concentrations of soluble $Fe^{2+}$ can be toxic (Chakraborty et al. 2013). Iron cycling in nature is dependent on biotic (microbial) and abiotic biogeochemical cycles (Pérez-Guzmán et al. 2010). Under aerated conditions and neutral or alkaline pH most Fe is in the insoluble ($Fe^{3+}$) form. Microbial activity and/or abiotic reactions reduce the redox potential resulting in the reduction of $Fe^{3+}$ to $Fe^{2+}$ (Pérez-Guzmán et al. 2010). Oxidation of iron in an aqueous media is known to decrease dissolved oxygen ($O_2$) concentrations and oxidation reduction potential (ORP) (Lin and Xing 2008) which can affect bacterial growth. Oxidative stress is the most commonly cited reason for the bactericidal property of NZVI (Jiang et al. 2015; Lee et al. 2008; Ludovica Sacca et al. 2013). The nanoparticles (NZVI) release $Fe^{2+}$ ions which generate reactive oxygen species (ROS) via Fenton's reaction (D.L. Wu et al. 2013b). The ROS can then react with microbial cell membrane lipids, proteins and DNA (Sevcu et al. 2011). The cytotoxic effects of NZVI on bacteria have been previously studied and are the result of the disruption of cell membrane integrity and respiratory activity caused by the generation of ROS (Auffan et al. 2008). This study aids in determining how the initial disruption of bacterial cells resulting from NZVI additions affects Fe uptake. Diao et al. (Diao and Yao 2009) observed that under aerobic conditions a concentration of 10 mg $mL^{-1}$ NZVI inactivated bacteria immediately. The half-life of NZVI in an aerobic environment is 35 s and inactivation of bacteria is due to the oxidation of NZVI that generates intercellular ROS with a high affinity for bacterial cells (Kim et al. 2010). Low concentrations (0.1 mg $mL^{-1}$ and 1 mg $mL^{-1}$) have also been shown to inactivate bacteria but at a slower rate (Diao and Yao 2009). However, this observation was made under vigorous shaking, which may also have resulted in the needle like NZVI penetrating and/or damaging the cell membrane of bacteria (Diao and Yao 2009).

Most gram-negative bacteria including *P. fluorescens* use a combination of siderophores, heme, transferrin and lactoferrin proteins to acquire Fe needed for growth (Krewulak and Vogel 2008). *P. fluorescens* acquires insoluble Fe by secreting siderophores (Chakraborty et al. 2013) and can reduce the expression of Fe proteins when Fe is bioavailable (Sacca et al. 2014). In such instances, Fe homeostatic machinery is expressed which ensures that Fe is acquired per the cell's needs and that intracellular levels of free Fe do not reach toxic levels (Lefevre et al. 2016). *P. fluorescens* uses the siderophore pyoverdin to chelate insoluble Fe(III) (Miethke and Marahiel 2007) and transport it into the bacteria via outer membrane receptors which bind to the $Fe^{3+}$ by utilizing the electrochemical charge of the cytoplasmic membrane. Ferric siderophore complexes are transported through the protein structure TonBExbB-ExbD with additional aid from the periplasmic binding protein and cytoplasmic membrane transporter. The ABC protein facilitates the transportation of ferric-siderophores into the cytoplasm where enzymes act on the complex to dissociate the Fe from the siderophore releasing ferrous Fe which can be used in various cellular metabolic processes (Krewulak and Vogel 2008; Vasil 2007).

Once Fe is in the cell and converted to the ferrous form, concentrations of $Fe^{2+}$ must be tightly regulated to prevent oxidative stress. Therefore, there is virtually no free Fe and most Fe in bacterial cells is bound to proteins. Excess Fe (II) in *P. fluorescens* cells would result in the production of reactive oxygen species such as superoxides ($O_2^{-}\cdot$) and hydroxyl radicals ($\cdot OH$) (Lim et al. 2012). Typically, bacteria convert excess cellular Fe (II) into Fe (III) via ferroxidase expression. In contrast, limited iron supply increases the transcription of *P. fluorescens*' iron acquisition system that regulates the expression of the *pvdS* gene. This gene is involved in the production of the siderophore pyoverdine used by *P. fluorescens* to chelate insoluble Fe exterior to the bacterial cells (Lim et al. 2012). An additional means of acquiring Fe under iron limited conditions is the mobilization of Fe stores from proteins within the bacteria such as bacterioferritin B (a protein that stores $Fe^{3+}$ as ferric hydroxyl phosphate) (Lim et al. 2012).

This research investigated the effects of varying concentrations of NZVI (1, 2 and 5 g $L^{-1}$) on the viability, growth, and iron acquisition by *P. fluorescens*. Microscale zero-valent iron (MZVI) particles were also included in this study to determine and compare the effects of particle size on Fe acquisition and use in *P. fluorescens*. In furtherance of these objectives, the siderophore production was measured using the blue agar CAS assay and transcription of mRNA from two genes involved in Fe utilization. Transmission electron microscopy (TEM) and Energy Dispersive X-ray Spectroscopy (EDS) were used to determine the location of NZVI and MZVI particles in and around the bacterial cells.

## 2. Experimental section

### 2.1. Materials

All chemicals and supplies were used as received from the suppliers unless otherwise specified.

### 2.2. Stock solutions and growth curves

Stock cultures for the project were grown from a freeze dried pure culture of *P. fluorescens* (ATCC® 13,525™, Manassas, VA, USA). Glycerol stocks of the *P. fluorescens* culture were stored in a −80 °C freezer until use. Cell counts were obtained for each stock culture to ensure that each treatment contained the same number of *P. fluorescens* at the start of the experiment. In addition, a loop of bacteria was taken from each stock culture and streaked on to a separate King B agar plate to verify the purity of the culture. King B agar was developed as a selective media for *P. fluorescens* and only *P. fluorescens* colonies grown on the agar emit a green fluorescence when exposed to a UV lamp. The media consisted of proteose peptone (20.0 g $L^{-1}$), glycerol (10 mL $L^{-1}$), $K_2HPO_4$ (1.5 g $L^{-1}$), $MgSO_4$ (1.5 g $L^{-1}$) and agar (15.0 g $L^{-1}$).

*P. fluorescens* was added at a concentration of $10^4$ CFU $mL^{-1}$ ($10^4$ cells $mL^{-1}$) to sterile tubes containing 20 mL of tryptic soy broth (TSB) to measure growth curves and rates for the bacterial control and bacterial treatments exposed to NZVI concentrations of 1, 2 and 5 g $L^{-1}$. The components of TSB in DI water were tryptone (17.0 g $L^{-1}$), soytone (3.0 g $L^{-1}$), glucose (2.5 g $L^{-1}$), sodium chloride (5.0 g $L^{-1}$) and dipotassium phosphate (2.5 g $L^{-1}$). After adding NZVI to the broth, the solution was sonicated and bacteria were added to the broth. Controls included TSB broth or NZVI and TSB at concentrations of 1, 2 or 5 g $L^{-1}$ with no bacteria. The growth curve was used to determine the viability of cells after treatment with variable doses of NZVI. Cultures exposed to MZVI were all viable and were not included in the growth curve experiment but were included in experiments to determine the mechanisms involved in Fe acquisition. All treatments and controls were replicated three times at each time interval (0, 6, 12, 18, 24, 30 and 48 h). Tubes were incubated at 30 °C on a rotating incubator

shaker at 180 rpm. One milliliter aliquots were taken at all time intervals and serially diluted for plate counts. One hundred microliters of each diluted bacterial solution was used to inoculate TSB agar plates in triplicate. The plates were incubated at 30 °C for 48 h and colonies were counted. The triplicate CFU values for each time interval by treatment were plotted to obtain a growth curve. To rule out contamination at each time interval, when aliquots were removed, a loop of bacteria was taken from several tubes and each loop streaked on to a separate *P. fluorescens* selective King B agar plate.

### 2.3. Preparations of NZVI

Iron nanoparticles (NPs) were synthesized via the sodium borohydride reduction of ferrous ion ($FeSO_4.7H_2O$) in an aqueous phase ($2Fe^{2+} + BH_4^- + 3H_2O \rightarrow 2Fe^0\downarrow + H_2BO_3^- + 4H^+ + 2H_2$) (Bezbaruah et al. 2009; Krajangpan et al. 2012; Li et al. 2006). The synthesized NZVI NPS were dried overnight in a vacuum under flowing $N_2$. The dried NZVI NPs were than air-stabilized (passivated) for 12 h and stored in sealed vials (headspace flushed with $N_2$ gas). The particles were characterized using TEM-EDS and the size distribution was recorded after ImageJ analysis. The surface area of the particles was measured using a BET surface area analyser.

### 2.4. pH and ORP

pH and oxidation reduction potential (ORP) were measured for all the samples and time intervals when aliquots were removed for the growth curve studies. pH and ORP were also measured in the samples treated with MZVI. Samples included TSB with bacteria treated with NZVI and MZVI (both 1, 2 and 5 g $L^{-1}$), and controls (TSB broth with bacteria and no Fe particles and TSB broth (no bacteria and Fe particles). ORP values were measured with an Ag/AgCl reference electrode, normalized to pH 7, and converted to $E_h$ (ORP vs Hydrogen reference electrode) for reporting.

### 2.5. Chrome azurol S (CAS) plates

The Blue Agar CAS assay of Louden et al. (Louden et al. 2011) adapted from Schwyn and Neilands (Schwyn and Neilands 1987) was used to detect siderophore production. The detailed procedure is presented elsewhere (MethodsX paper, Fortuna et al.).

If there were insufficient viable *P. fluorescens* cells for regrowth on CAS agar plates (e.g., 2 and 5 g $L^{-1}$ NZVI), these treatments are not included in the blue agar CAS assay data set. Plates were incubated with 100 µL of bacteria grown for 24 h in the presence of 1 g $L^{-1}$ NZVI and 1, 2 or 5 g $L^{-1}$ additions of MZVI. Controls included TSB broth with bacteria and TSB broth with NZVI and MZVI (1, 2 and 5 g $L^{-1}$) without bacteria. Internal controls were run with known concentrations of desferal, a chelating agent, derived from deferoxamine mesylate salt ($C_{26}H_{52}N_6O_{11}S$) (BioVision Inc., Milpitas, CA) dissolved in water and pipetted on to CAS agar plates per the method of Shin et al.(Shin et al. 2001).

### 2.6. qRT-PCR method

The viable *P. fluorescens* cell numbers in cultures treated with 2 and 5 g $L^{-1}$ NZVI (blue agar CAS assay experiment) were insufficient to extract and quantify mRNA. Messenger ribonucleic acid (mRNA) was isolated from the bacterial control, 1 g $L^{-1}$ NZVI with bacteria at the 24 h time interval of the growth curve and the 1 and 2 g $L^{-1}$ MZVI bacterial treatments at 24 h. Tubes of TSB broth were inoculated with bacteria and each respective MZVI treatment rate (1 and 2 g $L^{-1}$ MZVI) on Day 1 and samples were incubated for 24 h prior to mRNA extraction. All treatments were run in triplicate. *P. fluorescens* RNA was isolated using the UltraClean® Microbial RNA Isolation Kit (MOBIO Laboratories Inc., Carlsbad, CA) and purified with Ambion® DNA-free™ DNase Treatment and Removal Reagents (MOBIO Laboratories Inc., Carlsbad, CA). The SuperScript® VILO™ cDNA Synthesis Kit was used to synthesize cDNA from mRNA (Invitrogen, Grand Island, NY).

The primers used in the qRT-PCR analysis to isolate genes that regulate Fe acquisition in *P. fluorescens* were adapted from primers designed for a microarray by Lim et al. (2012). The two primer pairs synthesized amplified a 145 bp fragment of the *pvdS* gene, PFL_4190-qF *pvdS* CAGATCACCTCCTCGTTCAA and PFL_4190-qR *pvdS* CGCCATGA ATAACCACATTC, and a 172 bp fragment of the bacterioferritin-associated ferredoxin gene, PFL_4858-qF ferredoxin CGACGGACAAATTCG CGAAGCG and PFL_4858-qR ferredoxin CACAGGGTAGGGGATTGCCGC (Invitrogen, Carlsbad, CA). Master mixes and thermocycler conditions (PikoReal system, Thermo Scientific, Wilmington, DE) were held constant for the two primer pairs. The detailed procedure is presented elsewhere (MethodsX paper, Fortuna et al.). R-squared values were 0.99. Genomic DNA isolated from organismal controls and cDNA from TSB samples were run in triplicate. Standard curves were generated using genomic DNA isolated from *Pseudomonas fluorescens* Migula (ATCC® BAA-477D™, Manassas, VA).

### 2.7. Statistical analysis

Individual treatment effects ($P < 0.01$) were analyzed across time intervals between the control and 1 g $L^{-1}$ growth curves using analysis of variance in a completely randomized factorial design and Fisher LSD test. Individual treatment effects ($P < 0.01$) were also analyzed across time intervals 18, 24 and 30 h and between *P. fluorescens* treatments grown in the presence of 2 and 5 g $L^{-1}$ NZVI. Growth was insufficient to develop growth curves for these treatments. Individual treatment effects ($P < 0.0001$) at the 24 h time interval were analyzed via analysis of variance using the SAS PROC GLM procedure and Fisher LSD testing ($P < 0.01$) in SAS 9.4 (SAS Institute, Cary, NC). The NZVI treatments are not shown here because there was no measurable gene expression in the presence of 1 g $L^{-1}$ NZVI and in the 2 and 5 g $L^{-1}$ treatments there was insignificant microbial growth.

### 2.8. Transmission electron microscopy (TEM) and energy loss and energy dispersive spectroscopy (EDS)

For TEM, *P. fluorescens* containing samples that had been centrifuged to form pellets were agitated to resuspend the bacteria, then fixed in 2.5% glutaraldehyde in 0.1 M sodium phosphate buffer (pH 7.35, Tousimis Research Corporation, Rockville MD) for 1 h at 4 °C. Between each of the following steps, bacteria were agitated to resuspend, then centrifuged for 5 min at 10,000 rpm. Samples were rinsed twice in sodium phosphate buffer and then placed in 2% osmium tetroxide in buffer for 2 h at room temperature (22 ± 2 °C). Following buffer rinse, water rinse, and dehydration through a graded acetone series (0–30–50-70% acetone in water), pellets were stained en bloc with saturated uranyl acetate in 70% acetone for 3 h, then further dehydrated through two changes of 100% acetone. Dehydrated samples were embedded in Epon-Araldite-DDSA with DMP-30 accelerator polymerized in a 60 °C oven for 24 h and sectioned at 60–80 nm thickness on a RMC MT XL ultramicrotome (Boeckeler Instruments, Tucson AZ). Sections were collected on copper grids. Imaging and analysis were performed on a JEOL JEM-2100 $LaB_6$ transmission electron microscope (JEOL USA, Peabody MA) operating at 200 kV. Bright-field images of each sample were acquired with a Gatan Orius SC1000 CCD camera; dark-field imaging utilized a Gatan 805 High Angle Annular Dark Field detector with a Gatan Digiscan II controller unit and the TEM running in scanning transmission electron microscopy mode. A Thermo Nanotrace Energy Dispersive X-ray detector with NSS-212e acquisition engine integrated with the dark-field scanning TEM system was used to obtain X-ray information.

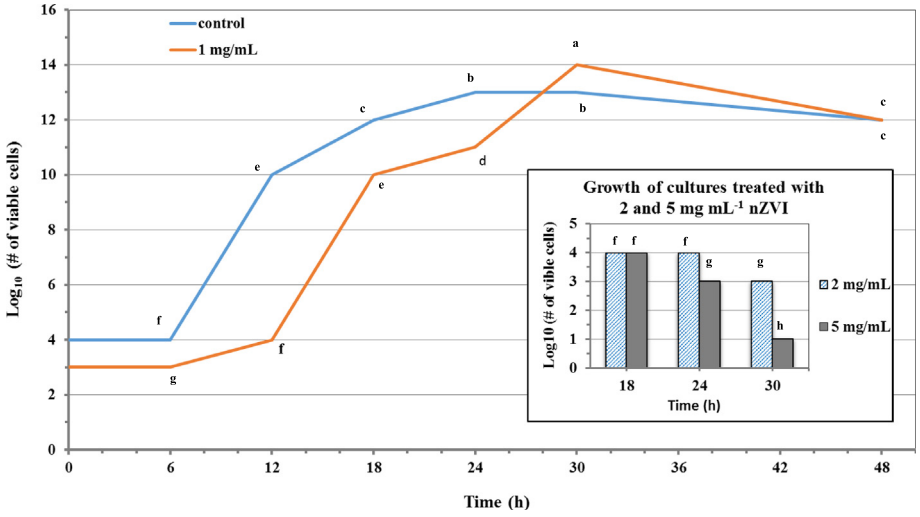


**Fig. 1.** Growth curves for *Pseudomonas fluorescens* with no NZVI additions (control) and in the presence of 1 g $L^{-1}$ (mg $mL^{-1}$) NZVI. Individual treatment effects ($P < 0.01$) were analyzed across time intervals between the growth curves using analysis of variance in a completely randomized factorial design and Fisher LSD test. (Inset: Individual treatment effects ($P < 0.01$) were also analyzed across time intervals 18, 24 and 30 h and between *P. fluorescens* treatments grown in the presence of 2 and 5 g $L^{-1}$ (mg $mL^{-1}$) NZVI. Growth was insufficient to calculate growth curves for these treatments.)

## 3. Results and discussion

### 3.1. Characterization of iron particles

The particle size (diameter) of the synthesized nanoparticles (Figs. S1a-b) was within the nano range (< 100 nm, average = 35 nm), and had a specific surface area of 25 $m^2$. Microscale zero-valent iron (MZVI) particles were purchased from a vendor (Aldrich) and had a specific surface area of 2 $m^2$ $g^{-1}$.

### 3.2. Growth curves

In order to study the impact of NZVI on *P. fluorescens*, growth curves were plotted using the plate count data (Fig. 1). The growth curve for the control (*P. fluorescens* without NZVI addition) revealed a 6 h lag phase, followed by a log phase from 6 to 24 h, a stationary phase at 24 h and death by 30 h. Bacterial growth in the 1 g $L^{-1}$ NZVI treatment was significantly greater than that of the control (Fig. 1). Specifically, the lag phase had ended by 6 h and cell growth occurred between 12 and 30 h after which bacteria began to die. Colony forming units (CFU) on 30 h at the end of the growth phase were significantly higher in the bacterial cultures treated with 1 g $L^{-1}$ NZVI relative to the bacterial control ($P = 0.01$) at 24 h and 30 h. The highest CFU value for the *P. fluorescens* control occurred at 24 h ($10^{13}$ CFU $mL^{-1}$) whereas bacteria treated with 1 g $L^{-1}$ NZVI had significantly higher CFUs at 30 h ($10^{14}$ CFU $mL^{-1}$). The 10-fold increase in bacterial cell counts in the presence of 1 g $L^{-1}$ NZVI suggests that the NZVI may be utilized as nutrient by *P. fluorescens*. In contrast, few or no *P. fluorescens* cells survived or were viable after addition of 2 and 5 g $L^{-1}$ NZVI. Both treatments showed a prolonged lag phase of ~18 h at which time bacterial counts were no greater than the initial cell numbers added to the TSB ($10^4$ CFU, highest for the two treatments) after which CFUs did not increase and bacterial growth showed declines. Growth curves could not be generated for these treatments due to insufficient numbers of viable cells. Other researchers have shown that the concentration of NZVI toxic to bacteria depends upon the strain and environmental conditions but is typically in the range of 1 to 10 g $L^{-1}$ (Diao and Yao 2009; Fajardo et al. 2013; Lefevre et al. 2016; Mitrano et al. 2015; Sacca et al. 2014).

As NZVI particles were oxidized cell membrane disruption occurs as a result of the production of $Fe^{2+}$ and ROS (Lefevre et al. 2016). Our results indicate that the majority *P. fluorescens* cells in the 2 and 5 g $L^{-1}$ treatments were destroyed or damaged after NZVI was added, preventing the cells from replicating. The authors hypothesized that measured increases in CFUs associated with the 1 g $L^{-1}$ NZVI treatment resulted from the bacteria's ability to utilize the Fe as a micronutrient. Others have also reported increased bacterial growth in the presence of low NZVI concentrations (0.56 g $L^{-1}$) (Chen et al. 2013). To validate the hypothesis, the authors collected additional measurements in an effort to verify uptake of Fe derived from NZVI by bacteria via CAS plates, qRT-PCR and EDS (see results in the proceeding sections).

### 3.3. pH and ORP value

ORP and pH of the TSB receiving various treatments were measured (Fig. 2 and SI, Fig. S2) at different NZVI concentrations in the presence or absence of *P. fluorescens*. The pH of the TSB broth containing bacteria alone varied from 6.7 to 7.2 and the $E_h$ values (initial +291.4 mV) were positive until 30 h (the end of the stationery phase) at which time the $E_h$ values remained negative. The positive $E_h$ values during 0 to 30 h in the control indicated that the media remained aerobic although the $E_h$ decreased due to the consumption of $O_2$ by *P. fluorescens* for cell growth. The pH value in the 1 g $L^{-1}$ NZVI (no bacteria) treatment varied from 7.3 to 8.1 while the $E_h$ increased from −1.1 mV ($t = 0$ h) to +331.1 mV ($t = 6$ h) and remained positive until the final measurement (+270 mV, $t = 48$ h). The initial negative $E_h$ value implies that when the NZVI particles were added to the TSB media, the nanoparticles immediately reacted with the TSB and were oxidized resulting in a reducing ($O_2$ deficient) environment. A similar trend was observed in the 1 g $L^{-1}$ NZVI with bacteria treatment with $E_h$ values of −1.1 mV (0 h) and +315.7 mV at the end of the lag phase ($t = 12$ h) and remained high (+261.7 mV) until 24 h and positive until 30 h.

Although, the optimal pH for *P. fluorescens* growth is reported to be 7.2 and optimal ORP (as $E_h$) is +123 mV (Buddingh 1974), *P. fluorescens* is an aerobe and a facultative anaerobe that typically persists across a range of $E_h$ values from as high as +200 mV ($3.8 \times 10^8$ CFU) to as low as +40 mV ($10^6$ CFU) (Tabatabai and Walker 1970). In the current study, the pH (~7.0) and $E_h$ (+511 mV at t = 0 h and +440 mV at t = 48 h) of TSB media without bacteria or NZVI remained more or less constant.

Our data and those of others verify that bacteria can persist briefly at ORP lower than optimum (Diao and Yao 2009; Fajardo et al. 2013; Lefevre et al. 2016; Mitrano et al. 2015; Sacca et al. 2014; Tabatabai and Walker 1970). In addition, ORP and to a lesser degree pH determine the species and mineral associated Fe present in the TSB broth and that in turn determines the bioavailability of the Fe in the NZVI. Once introduced to the broth, NZVI particles oxidized, redox conditions equilibrated and elemental Fe(0) was converted to forms of iron oxides and hydroxides reducing the toxicity (Elliott et al. 2009; Kumar et al. 2014a; Lefevre et al. 2016; Sacca et al. 2014). The redox environment in

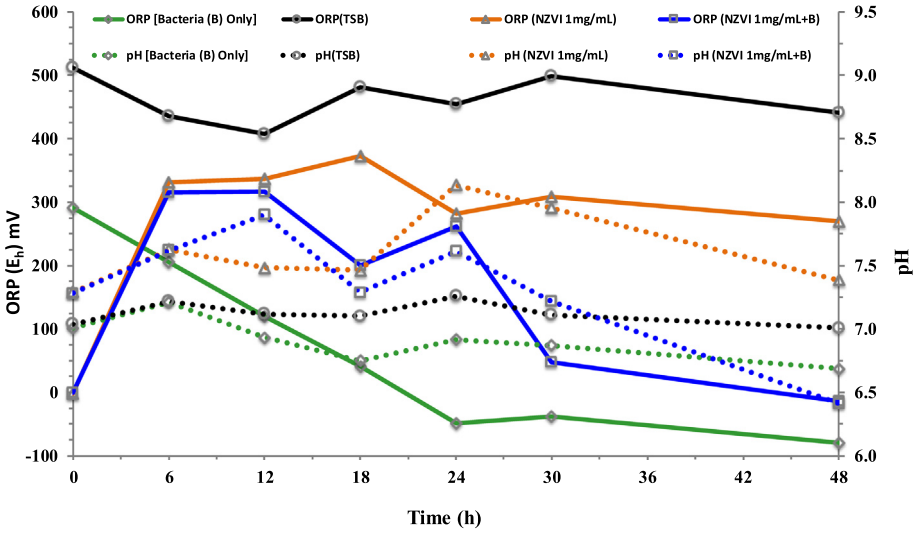


**Fig. 2.** pH and oxidation-reduction potential (ORP as $E_h$) changes over time for 1 g $L^{-1}$ (mg $mL^{-1}$) NZVI in tryptic soy broth (TSB) in the presence and absence of *Pseudomonas fluorescens*. The pH and ORP plots for control (only bacteria with no NZVI) and only TSB solution are presented for comparison.

the TSB broth shifted from anaerobic to aerobic (favoring bacterial growth) prior to the 6 h time interval in the 1 g $L^{-1}$ NZVI treatment with and without bacteria. In contrast to that of the 1 g $L^{-1}$ NZVI without bacteria treatment, $E_h$ decreased for a second time in the 1 g $L^{-1}$ NZVI treatment containing bacteria. The decrease in ORP corresponded with increases in bacterial respiration and growth as was the case of the bacterial control without NZVI addition in which the ORP was +261 mV at 24 h and decreased to +48 mV at 30 h at the end of the log phase.

The low (−2 mV) redox conditions (immediately after NZVI addition) resulted in the extended lag phase seen in the 1 g $L^{-1}$ with bacteria treatment and the lack of growth in the 2 and 5 g $L^{-1}$ treatments. Although the $E_h$ values in the 2 g $L^{-1}$ with bacteria treatment were positive after 6 h and the pH was conducive (7.3–8) for bacterial growth, the initial very reductive reduction condition (−32 mV) due to the addition of the NZVI in this treatment permanently reduced the number of bacterial cells that would have otherwise reproduced throughout the duration of the experiment. The lower $E_h$ values (−42 to −119 mV) in the 5 g $L^{-1}$ treatment with bacteria reflected the anaerobic conditions that persisted during the growth curve experiment in contrast to the aerobic environment in the 1 g $L^{-1}$ treatment with bacteria after the 12 h lag phase. These mostly anaerobic $E_h$ ranges resulted in conditions that did not favor bacterial survival and growth. Anaerobic $E_h$ values increase concentrations of $Fe^{2+}$ to toxic levels (Lefevre et al. 2016). Others have reported higher ROS production from Fe(0) under low redox conditions (Lee et al. 2008) and that might have been the primary cause of bacterial death in 2 and 5 g $L^{-1}$ treatments.

Treatments containing bacteria exposed to MZVI had lower pH values (6.4–7.3 for 1 g $L^{-1}$, 6.4–7.4 for 2 g $L^{-1}$, 7–7.5 for 5 g $L^{-1}$) and positive initial ORP values (> +400 mV). The initial positive $E_h$ values and near neutral pH supported bacterial growth. Based on these redox and pH results and existing literature (Lee et al. 2008), it can be inferred that the greater surface area of the NZVI resulted in the production of ROS at toxic levels relative to an equivalent mass of MZVI. Kim et al. (Kim et al. 2010) found that NZVI has a higher affinity for bacterial cells relative to $Fe^{2+}$ at pH 7. This affinity may increase the concentration of $Fe^{2+}$ that can be utilized by bacterial cells. In addition, other researchers have demonstrated that the greater affinity of NZVI to sorb to cell membranes results in the inhibition of nutrient uptake and damages the structure of the bacterial cell membrane (Stefaniuk et al. 2016). Cell death was the result of initial NZVI additions to *P. fluorescens* cultures. Although significant cell death occurred initially in cultures treated with 1 g $L^{-1}$ NZVI after a 12 h lag in cell growth, sufficient cells remained and conditions in the culture (ORP, pH and Fe availability) favored increased growth of *P. fluorescens* after the lag phase.

### 3.4. CAS plate

The CAS plate method was successfully used to detect siderophore production (pyoverdins). When the bacteria are grown under iron limiting conditions, an orange to yellow halo forms around *P. fluorescens* colonies which confirms the bacteria are Fe limited and secreting siderophores to chelate essential iron. The presence or absence of siderophore secretion also provided insight with respect to the bioavailability of NZVI to bacteria. *P. fluorescens* cells exposed to 2 and 5 g $L^{-1}$ were nonviable or damaged and failed to grow on CAS agar. The largest halo was formed around colonies containing pure cultures of the bacteria supplied with no Fe (control treatment, see the MethodsX paper, Fortuna et al.). Similarly, in MZVI treatments, siderophore production was observed (see the MethodsX paper, Fortuna et al.) but the diameter of the halos (in mm) was smaller than those in the control. In contrast, colonies grown in the presence of 1 g $L^{-1}$ NZVI developed the smallest halo which suggests the production of siderophores were reduced relative to bacteria grown in the presence of MZVI due to their potential acquisition of Fe from the 1 g $L^{-1}$ NZVI in the media. After comparing the results from NZVI and MZVI, it is safe to infer that the size (specific surface area) of Fe particles played a critical role in Fe utilization by *P. fluorescens*. Iron dissolution studies indicate that for the time points for which the CAS plate were studied (until 30 h), NZVI (1 g $L^{-1}$) dissolution has very high (118–300 mg $L^{-1}$ at 6–30 h) and it was low (11–97 mg $L^{-1}$ at 6–30 h) for MZVI (1 g $L^{-1}$) (Fig. S3; also see the MethodsX paper, Fortuna et al.). The authors relate the high reactive surface area in NZVI (25 $m^2$ $g^{-1}$, compared to 2 $m^2$ $g^{-1}$ for MZVI) as the main reason for this high dissolution rate.

### 3.5. qRT-PCR

The increase in bacterial growth counts and lack of siderophore secretion on CAS agar plates in the 1 g $L^{-1}$ NZVI treatment with bacteria relative to the control indicated that *P. fluorescens* may be utilizing the NZVI as a source of Fe. In contrast, there was insufficient growth of *P. fluorescens* in the 2 and 5 g $L^{-1}$ treatments to allow for extraction of mRNA. In the pure *P. fluorescens* culture treatment, both genes (*pvdS* (PFL 4190) and pyoverdine bacterioferritin-associated ferredoxin (PFL 4858)) were expressed indicating that under conditions where no Fe

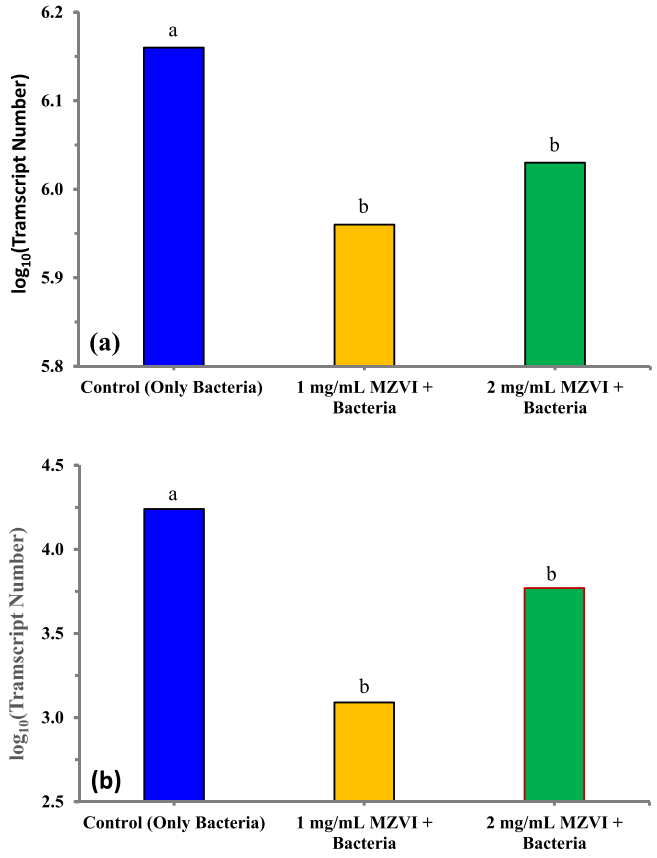


**Fig. 3.** mRNA expression levels of **(a)** the bacterioferritin-associated ferredoxin gene (PFL 4858), involved in mobilization and storage of Fe from bacterioferritin B, standard deviation ( ± 0.02) and (**b**) *pvdS* gene (PFL 4190), one of a cluster of genes regulating synthesis of siderophores ( ± 0.19) determined by qRT-PCR. The control bacteria treatment represents the *P. fluorescens* culture without Fe addition. Treatments 1 g $L^{-1}$ (mg $mL^{-1}$) MZVI + Bacteria and 2 mg $mL^{-1}$ MZVI + Bacteria represent *P. fluorescens* cultures grown in the presence of 1 and 2 g $L^{-1}$ (mg $mL^{-1}$) MZVI, respectively. The genes were not expressed in the *P. fluorescens* culture treated with 1 mg $mL^{-1}$ NZVI possibly because of the bioavailability of Fe from the NZVI in this treatment. Individual treatment effects ($P < 0.0001$) at the 24 h time interval were analyzed via analysis of variance using the SAS PROC GLM procedure and Fisher LSD testing ($P < 0.01$) in SAS 9.4 (SAS Institute, Cary, NC). Note: The NZVI treatments are not shown here because there was no measurable gene expression in the presence of 1 g $L^{-1}$ (mg $mL^{-1}$) NZVI and in the 2 and 5 g $L^{-1}$ (mg $mL^{-1}$) treatments there was insignificant microbial growth.

supplement was introduced, bacteria utilized their Fe reservoirs and solubilized insoluble Fe to meet their Fe requirement (Figs. 3a-b). These results also clearly revealed that addition of NZVI to bacterial cultures at the 1 g $L^{-1}$ concentration led to neither gene being expressed. Hence, the *P. fluorescens* were likely utilizing NZVI as a Fe source and did not need to produce siderophores or utilize Fe stores in the cell. Down regulation decreases the production of proteins in cell membranes associated with porins, proteins that form a pore that allows for transport across the cell membrane Earlier studies have reported that the presence of NZVI results in reduction in expression of genes involved in Fe acquisition to prevent excessive uptake (Mohanty et al. 2015; Sacca et al. 2014).

Expression of the bacterioferritin-associated ferredoxin (PFL 4858) gene was similar. Gene transcription was significantly greater (Fig. 3a, $P < 0.0001$) in the *P. fluorescens* control culture receiving no Fe addition relative to the treatments grown in the presence of 1 and 2 g $L^{-1}$ MZVI. The MZVI particle treatment verified that the size of the Fe played a role in Fe uptake. In the 1 and 2 g $L^{-1}$ MZVI treatments, the *pvdS* gene was expressed but its transcription was significantly lower relative to the untreated bacterial control (Fig. 3b, $P < 0.0001$). Iron concentrations in bacterial cells are tightly regulated by the cell than siderophore production (Guerinot 1994) which would explain the similarity in expression of the bacterioferritin-associated ferredoxin (PFL 4858) gene. Our data indicate that much of the MZVI was insoluble requiring the production of siderophores to chelate and transport the Fe into the bacterial cells. In addition, utilization of Fe from protein stores in bacterial cells verified that the majority of MZVI at either concentration was not being utilized by *P. fluorescens* in these treatments. Treatment of bacterial cultures with 1 g $L^{-1}$ NZVI significantly reduced siderophore production, expression of genes associated with Fe acquisition and significantly increased growth of *P. fluorescens* relative to the untreated bacterial control and MZVI treatments containing bacteria.

### 3.6. TEM and EDS

In order to determine the effect of NZVI on bacterial cells and to verify the uptake and location of Fe added, TEM and EDS analyses were performed. The qRT-PCR results indicated that *P. fluorescens* transcriptional levels of genes associated with Fe acquisition were below the threshold for detection in NZVI treatments but detectable with MZVI additions. The CAS agar assay corroborated our qRT-PCR results, providing additional evidence that with Fe acquisition was suppressed by NZVI but not MZVI. Specifically, there was no evidence that *P. fluorescens* cells produced siderophores after treatment with 1 g $L^{-1}$ NZVI while bacterial cultures exposed to MZVI continued to produce siderophores when regrown on CAS agar media. These results indicate that the bioavailability of NZVI is greater than that of MZVI. Therefore, we expected to find Fe derived from NZVI in the interior of cells grown in the presence of 1 g $L^{-1}$ NZVI.

TEM and EDS analysis obtained from *P. fluorescens* cells at 24 h in the MZVI treatment confirmed there was no Fe accumulation in the interior of cells (SI, Fig. S4). TEM and EDS analysis from bacteria grown in the presence of 1 g $L^{-1}$ NZVI contained greater numbers and more distinct extracellular polymeric substances (EPS) and/or vesicles that contained Fe (Figs. 4 and 5). However, *P. fluorescens* cells treated with 1 mg $mL^{-1}$ NZVI contained Fe (Figs. 5b-d and 6a-d) associated with cell membranes and within cells in locations that included potential vacuoles that appeared to contain Fe derived from NZVI (locations #4 and #6 in Fig. 6a-b) at the 24 h time interval (log phase of growth).

Vesicles can be formed in the presence of electropositive materials such as NZVI. Beveridge and Graham (Beveridge and Graham 1991) attributed the formations of similar structures to electropositive forces that displaced $Ca^{2+}$ and $Mg^{2+}$ from the lipopolysaccharide (LPS) resulting in “alteration of lipid packing order”. The change in LPS structure results in the formation of vesicles that protrude out of the cell membrane. The functions of EPS are highly variable and their numbers are dependent upon abiotic and biotic conditions (Beveridge and Graham 1991; More et al. 2014; Wolfaardt et al. 1999). EPS are involved in the production of bacterial biofilms, aggregation, nutrient transfer and retention and determine the hydrophilic/hydrophobic properties of the cells (Beveridge and Graham 1991; More et al. 2014). EPS accumulate metals such as Fe (Wolfaardt et al. 1999) and are coated with fine grain mineral Fe formations in our experiment (Fig. 4a-d) and that Fe could possibly be utilized by *P. fluorescens*. Beveridge and Graham (Beveridge and Graham 1991) suggested that bacteria have evolved in part to form such metal coatings and that this tendency has had a profound effect on nutrient cycling for millennium.

Nutrient concentrations that are insufficient or in excess have previously been shown to affect morphological properties of bacteria such as lysis and plasmolysis of cells, as well as the presence of vacuoles and EPS (Persson et al. 1990). Exopolysaccharides function as a defense against environmental stress such as high metal concentrations (Wolfaardt et al. 1999). Several other researchers have verified this effect and suggested that mineral coatings can block uptake by bacterial

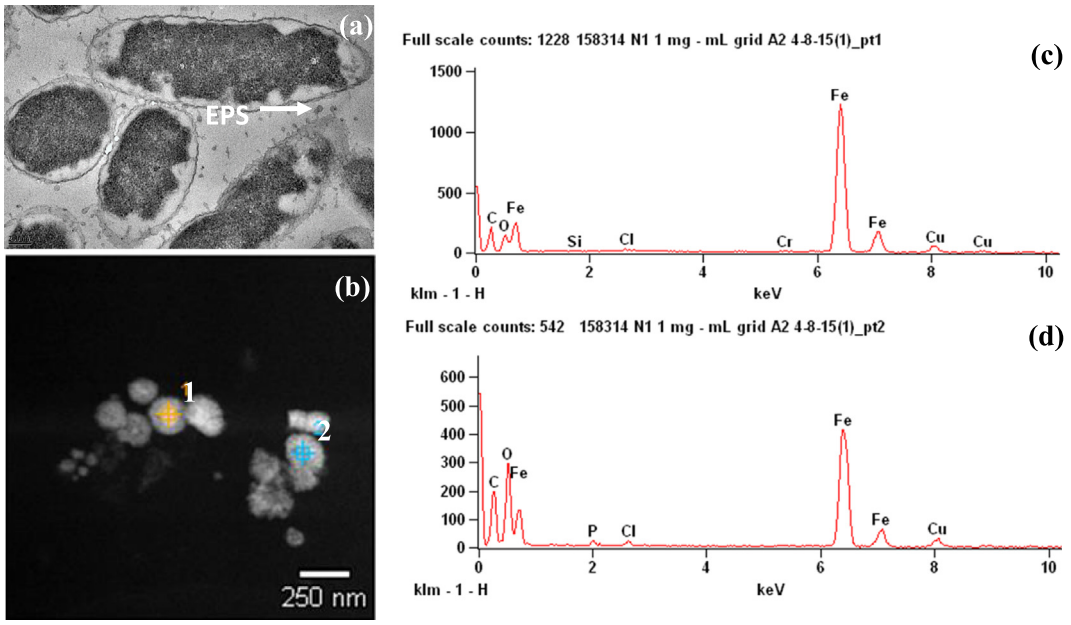


**Fig. 4.** TEM images of *Pseudomonas fluorescens* cells treated with 1 g $L^{-1}$ (mg $mL^{-1}$) NZVI. **(a)** Extracellular polymeric substances (EPS) are visible; **(b)** Mineral precipitates derived from the initial NZVI addition are visible; **(c)** and **(d)** EDS was performed in areas highlighted (#1 and #2) and Fe was observed [EDS at #1 is in (c), and EDS at #2 is in (d).]

porins (Stefaniuk et al. 2016). The EDS analyses in this experiment confirmed that while there was some Fe associated with the exterior of the cell, the interior of cells treated with 1 g $L^{-1}$ NZVI contained higher Fe concentrations (Fig. 5a-d). Thus, our research verifies that the fine grain mineral Fe formations and Fe derived from NZVI were at least partially utilized as a nutrient and did not appear to disrupt cell function after the initial NZVI addition (1 g $L^{-1}$). The TEM and EDS analyses confirmed that the interior of cells in the log phase of growth treated with 1 g $L^{-1}$ NZVI contained higher concentrations of Fe relative to the cell exterior and nutrient broth. This study determined that Fe species derived from NZVI in aqueous solution are potentially nutritive to the biota affect the growth and Fe acquisition of microorganisms.

### 3.7. Environmental significance

Much of peer-reviewed research addressing the environmental impact of nanomaterials including NZVI focuses on these materials' potential toxicity. However, there is growing evidence that nanomaterials

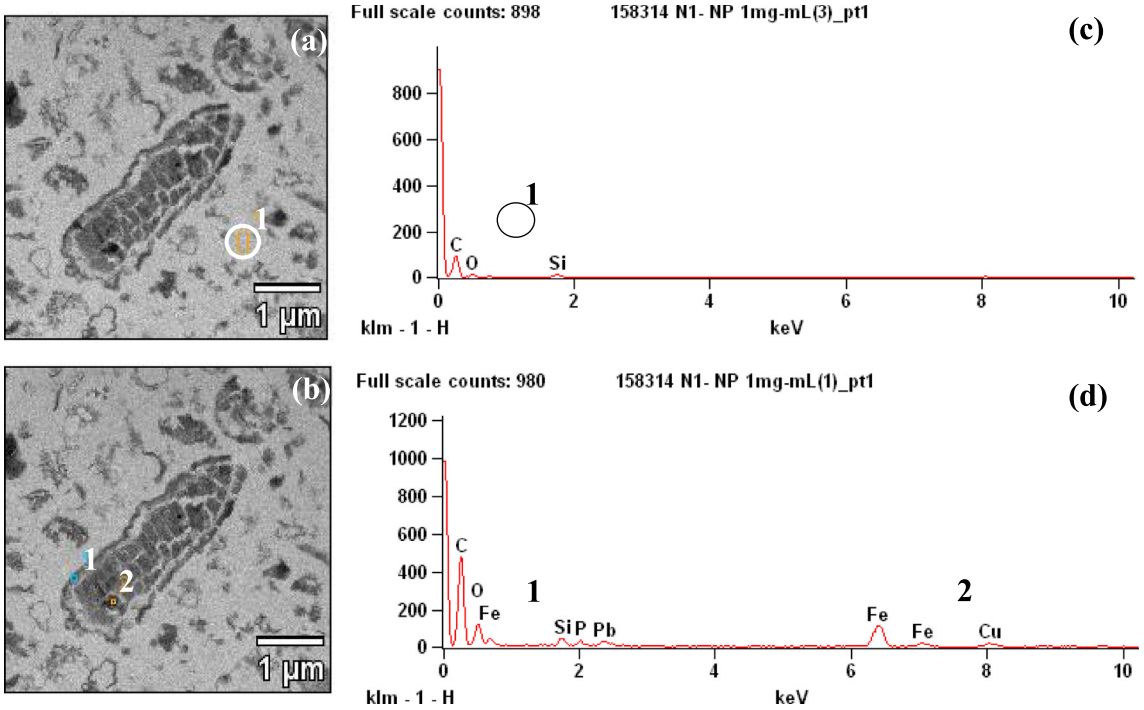


**Fig. 5. (a)** and **(b)** TEM images of a *Pseudomonas fluorescens* cell treated with 1 g $L^{-1}$ (mg $mL^{-1}$) NZVI; **(c)** EDS was done on the circled (#1) area in (a) and no Fe was detected in this area which was external to the cell; **(d)** EDS was done in highlighted areas (#1 and #2) and Fe was observed in these areas which were inside the bacterial cell.

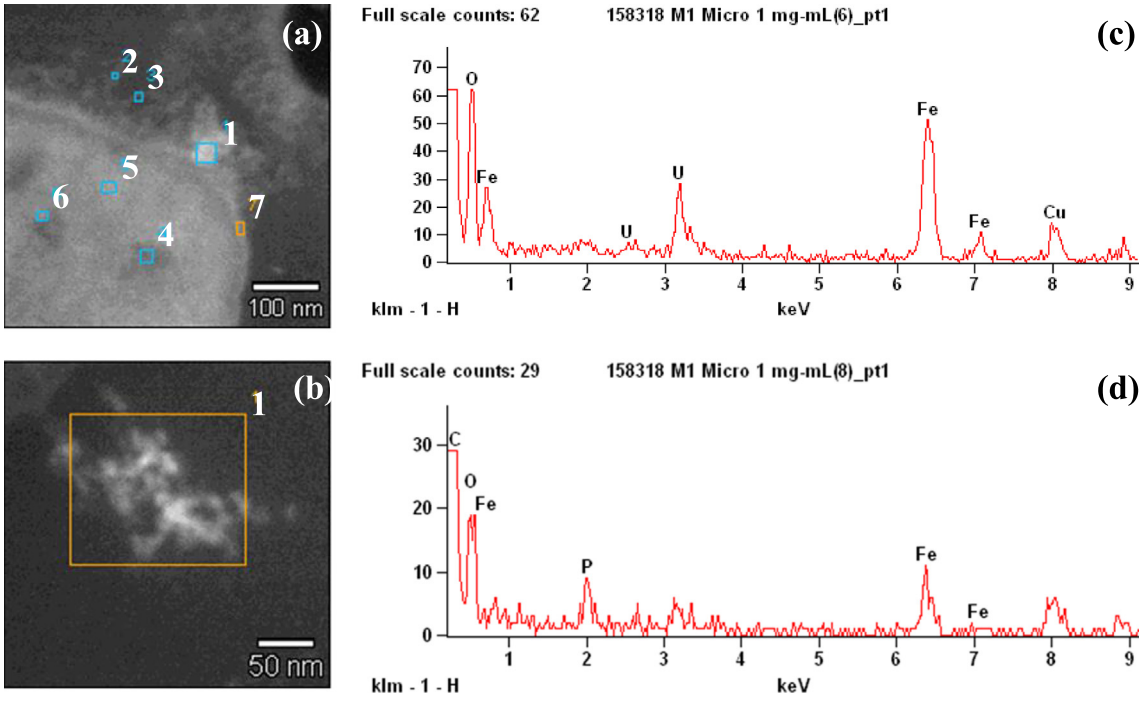


**Fig. 6. (a)** TEM images of a *Pseudomonas fluorescens* cell treated with 1 g $L^{-1}$ (mg $mL^{-1}$) NZVI. **(a)** EDS was done in the areas highlighted (numbered 1 through 7). The areas where Fe observed includes #1 (EPS), #4 and #6 (potential vacuoles that appear to contain Fe derived from NZVI), and #7 (cell membrane); **(b)** Magnified image of #1 in (a); **(c)** EDS done at #7 in (a); **(d)** EDS done at #1 in (a) and (b).

such as NZVI can also serve as a nutrient resulting in higher growth rates of organisms and bioaccumulation of nano-derived materials in cells. Therefore, determining what processes and mechanisms control uptake and utilization of nano-sized micronutrients in a range of organisms and environments is critical. This research addresses the mechanisms of NZVI derived Fe uptake in *P. fluorescens*, a ubiquitous gram negative bacteria found globally across numerous environments. The microorganism's growth response, uptake and accumulation of Fe when grown in the presence of 1 g $L^{-1}$ NZVI suggests that NZVI has the potential for use as an agricultural fertilizer and for nutrient management in lakes and similar waterbodies. Additional research is needed to determine the fate of NZVI and its potential nutritive effects on the growth of microorganisms particularly in oligotrophic environments such as water bodies that are often Fe limited.

## Acknowledgements

Funding for this project was provided by National Science Foundation (NSF grant nos. CMMI-1125674 and CBET 1707093, PI: Bezbaruah). NDSU Advanced Imaging and Microscopy Core Laboratory, and NDSU Electron Microscopy Core Laboratory (supported by NSF grant no. CMMI-0821655) helped in microscopy and imaging conducted in this study. Any opinions, findings, and conclusions or recommendations expressed in this material are those of the author(s) and do not necessarily reflect the views of the National Science Foundation (NSF).

## Appendix A. Supplementary data

Further information is available with respect to: transmission electron micrograph of NZVI (Fig. S1); pH and oxidation reduction potential (Fig. S2); Iron ion dissolution from NZVI and MZVI in TSB medium (Fig. S3); TEM micrograph of *P. fluorescens* cells at 24 h in the MZVI treatment confirmed that there was no Fe accumulation in the interior of cells (Fig. S4).

Siderophore production in *Pseudomonas fluorescens* colonies grown on CAS agar plates and TEM micrograph of *Pseudomonas fluorescens* exposed to 1 g $L^{-1}$ MZVI are presented elsewhere (the MethodsX paper, Fortuna et al.). Supplementary data to this article can be found online at doi: https://doi.org/10.1016/j.impact.2018.08.009.

## References

Aitken, R.J., Chaudhry, M.Q., Boxall, A.B.A., Hull, M., 2006. Manufacture and use of nanomaterials: current status in the UK and global trends. Occup. Med. 56 (5), 300–306.

Almeelbi, T., Bezbaruah, A., 2012. Aqueous phosphate removal using nanoscale zero-valent iron. J. Nanopart. Res. 14 (7).

Almeelbi, T., Bezbaruah, A., 2014. Nanoparticle-Sorbed phosphate: Iron and phosphate bioavailability studies with Spinacia oleracea and Selenastrum capricornutum. ACS Sustain. Chem. Eng. 2 (7), 1625–1632.

Auffan, M., Achouak, W., Rose, J., Roncato, M.A., Chaneac, C., Waite, D.T., Masion, A., Woicik, J.C., Wiesner, M.R., Bottero, J.Y., 2008. Relation between the redox state of iron-based nanoparticles and their cytotoxicity toward *Escherichia coli*. Environ. Sci. Technol. 42 (17), 6730–6735.

Beveridge, T.J., Graham, L.L., 1991. Surface-layers of bacteria. Microbiol. Rev. 55 (4), 684–705.

Bezbaruah, A.N., Krajangpan, S., Chisholm, B.J., Khan, E., Bermudez, J.J.E., 2009. Entrapment of iron nanoparticles in calcium alginate beads for groundwater remediation applications. J. Hazard. Mater. 166 (2–3), 1339–1343.

Bruton, T.A., Pycke, B.F., Halden, R.U., 2015. Effect of nanoscale zero-valent iron treatment on biological reductive dechlorination: a review of current understanding and research needs. Crit. Rev. Environ. Sci. Technol. 45 (11), 1148–1175.

Buddingh, G.J., 1974. Bergey's Manual of Determinative Bacteriology, 8th edition. The American Society of Tropical Medicine and Hygiene, Oakbrook Terrace, IL (USA).

Chakraborty, R., Braun, V., Hantke, K., Cornelis, P., 2013. Iron Uptake in Bacteria With Emphasis on *E. coli* and *Pseudomonas*. Springer Science & Business Media.

Chen, Q., Li, J., Wu, Y., Shen, F.X., Yao, M.S., 2013. Biological responses of gram-positive and gram-negative bacteria to nZVI (Fe-0), $Fe^{2+}$ and $Fe^{3+}$. RSC Adv. 3 (33), 13835–13842.

Diao, M., Yao, M., 2009. Use of zero-valent iron nanoparticles in inactivating microbes. Water Res. 43 (20), 5243–5251.

Elliott, D.W., Lien, H.L., Zhang, W.X., 2009. Degradation of lindane by zero-valent iron nanoparticles. J. Environ. Eng. ASCE 135 (5), 317–324.

Fajardo, C., Sacca, M.L., Martinez-Gomariz, M., Costa, G., Nande, M., Martin, M., 2013. Transcriptional and proteomic stress responses of a soil bacterium *Bacillus cereus* to nanosized zero-valent iron (nZVI) particles. Chemosphere 93 (6), 1077–1083.

Guerinot, M.L., 1994. Microbial iron transport. Annu. Rev. Microbiol. 48, 743–772.

Jiang, C.H., Xu, X.P., Megharaj, M., Naidu, R., Chen, Z.L., 2015. Inhibition or promotion of biodegradation of nitrate by *Paracoccus* sp in the presence of nanoscale zero-valent iron. Sci. Total Environ. 530, 241–246.

Kim, J.Y., Park, H.J., Lee, C., Nelson, K.L., Sedlak, D.L., Yoon, J., 2010. Inactivation of *Escherichia coli* by nanoparticulate zerovalent iron and ferrous ion. Appl. Environ. Microbiol. 76 (22), 7668–7670.
Krajangpan, S., Kalita, H., Chisholm, B.J., Bezbaruah, A.N., 2012. Iron nanoparticles coated with amphiphilic polysiloxane graft copolymers: dispersibility and contaminant treatability. Environ. Sci. Technol. 46 (18), 10130–10136.
Krewulak, K.D., Vogel, H.J., 2008. Structural biology of bacterial iron uptake. Biochim. Biophys. Acta Biomembr. 1778 (9), 1781–1804.
Kumar, N., Auffan, M.l., Gattacceca, J.r.m., Rose, J.r.m., Olivi, L., Borschneck, D., Kvapil, P., Jublot, M., Kaifas, D., Malleret, L., 2014a. Molecular insights of oxidation process of iron nanoparticles: spectroscopic, magnetic, and microscopic evidence. Environ. Sci. Technol. 48 (23), 13888–13894.
Kumar, N., Omoregie, E.O., Rose, J., Masion, A., Lloyd, J.R., Diels, L., Bastiaens, L., 2014b. Inhibition of sulfate reducing bacteria in aquifer sediment by iron nanoparticles. Water Res. 51, 64–72.
Lee, C., Kim, J.Y., Lee, W.I., Nelson, K.L., Yoon, J., Sedlak, D.L., 2008. Bactericidal effect of zero-valent iron nanoparticles on *Escherichia coli*. Environ. Sci. Technol. 42 (13), 4927–4933.
Lefevre, E., Bossa, N., Wiesner, M.R., Gunsch, C.K., 2016. A review of the environmental implications of in situ remediation by nanoscale zero valent iron (nZVI): behavior, transport and impacts on microbial communities. Sci. Total Environ. 565, 889–901.
Li, X.Q., Elliott, D.W., Zhang, W.X., 2006. Zero-valent iron nanoparticles for abatement of environmental pollutants: materials and engineering aspects. Crit. Rev. Solid State Mater. Sci. 31 (4), 111–122.
Lim, C.K., Hassan, K.A., Tetu, S.G., Loper, J.E., Paulsen, I.T., 2012. The effect of iron limitation on the transcriptome and proteome of *Pseudomonas fluorescens* Pf-5. PLoS One 7 (6).
Lin, D.H., Xing, B.S., 2008. Root uptake and phytotoxicity of ZnO nanoparticles. Environ. Sci. Technol. 42 (15), 5580–5585.
Louden, B.C., Haarmann, D., Lynne, A.M., 2011. Use of blue agar CAS assay for siderophore detection. J. Microbiol. Biol. Educ. 12 (1), 51–53.
Ludovica Sacca, M., Fajardo, C., Nande, M., Martin, M., 2013. Effects of nano zero-valent iron on *Klebsiella oxytoca* and stress response. Microb. Ecol. 66 (4), 806–812.
Ludovica Sacca, M., Fajardo, C., Costa, G., Lobo, C., Nande, M., Martin, M., 2014. Integrating classical and molecular approaches to evaluate the impact of nanosized zero-valent iron (nZVI) on soil organisms. Chemosphere 104, 184–189.
Miethke, M., Marahiel, M.A., 2007. Siderophore-based iron acquisition and pathogen control. Microbiol. Mol. Biol. Rev. 71 (3), 413.
Mitrano, D.M., Motellier, S., Clavaguera, S., Nowack, B., 2015. Review of nanomaterial aging and transformations through the life cycle of nano-enhanced products. Environ. Int. 77, 132–147.
Mohanty, A., Liu, Y., Yang, L., Cao, B., 2015. Extracellular biogenic nanomaterials inhibit pyoverdine production in *Pseudomonas aeruginosa*: a novel insight into impacts of metal(loid)s on environmental bacteria. Appl. Microbiol. Biotechnol. 99 (4), 1957–1966.
More, T.T., Yadav, J.S.S., Yan, S., Tyagi, R.D., Surampalli, R.Y., 2014. Extracellular polymeric substances of bacteria and their potential environmental applications. J. Environ. Manag. 144, 1–25.
Pérez-Guzmán, L., Bogner, K.R., Lower, B.H., 2010. Earth's ferrous wheel. Nature Education Knowledge 3 (10), 32.
Persson, A., Molin, G., Weibull, C., 1990. Physiological and morphological-changes induced by nutrient limitation of Pseudomonas-fluorescens 378 in continuous culture. Appl. Environ. Microbiol. 56 (3), 686–692.
Sacca, M.L., Fajardo, C., Martinez-Gomariz, M., Costa, G., Nande, M., Martin, M., 2014. Molecular stress responses to nano-sized zero-valent iron (nZVI) particles in the soil bacterium *Pseudomonas stutzeri*. PLoS One 9 (2), 7.
Schwyn, B., Neilands, J.B., 1987. Universal chemical-assay for the detection and determination of siderophores. Anal. Biochem. 160 (1), 47–56.
Sevcu, A., El-Temsah, Y.S., Joner, E.J., Cernik, M., 2011. Oxidative stress induced in microorganisms by zero-valent iron nanoparticles. Microbes Environ. 26 (4), 271–281.
Shin, S.H., Lim, Y., Lee, S.E., Yang, N.W., Rhee, J.H., 2001. CAS agar diffusion assay for the measurement of siderophores in biological fluids. J. Microbiol. Methods 44 (1), 89–95.
Sleiman, N., Deluchat, V., Wazne, M., Mallet, M., Courtin-Nomade, A., Kazpard, V., Baudu, M., 2016. Phosphate removal from aqueous solution using ZVI/sand bed reactor: behavior and mechanism. Water Res. 99, 56–65.
Sleiman, N., Deluchat, V., Wazne, M., Mallet, M., Courtin-Nomade, A., Kazpard, V., Baudu, M., 2017. Phosphate removal from aqueous solutions using zero valent iron (ZVI): influence of solution composition and ZVI aging. Colloids Surf. A Physicochem. Eng. Asp. 514, 1–10.
Stefaniuk, M., Oleszczuk, P., Ok, Y.S., 2016. Review on nano zerovalent iron (nZVI): from synthesis to environmental applications. Chem. Eng. J. 287, 618–632.
Tabatabai, L.B., Walker, H.W., 1970. Oxidation-reduction potential and growth of Clostridium-perfringens and Pseudomonas-fluorescens. Appl. Microbiol. 20 (3) (441-+).
Tosco, T., Papini, M.P., Viggi, C.C., Sethi, R., 2014. Nanoscale zerovalent iron particles for groundwater remediation: a review. J. Clean. Prod. 77, 10–21.
Vasil, M.L., 2007. How we learnt about iron acquisition in Pseudomonas aeruginosa: a series of very fortunate events. Biometals 20 (3–4), 587–601.
Wolfaardt, G.M., Lawrence, J.R., Korber, D.R., 1999. Microbial extracellular polymeric substances. Springer, Berlin.
Wu, D., Shen, Y., Ding, A., Qiu, M., Yang, Q., Zheng, S., 2013a. Phosphate removal from aqueous solutions by nanoscale zero-valent iron. Environ. Technol. 34 (18), 2663–2669.
Wu, D.L., Shen, Y.H., Ding, A.Q., Mahmood, Q., Liu, S., Tu, Q.P., 2013b. Effects of nanoscale zero-valent iron particles on biological nitrogen and phosphorus removal and microorganisms in activated sludge. J. Hazard. Mater. 262, 649–655.
Yang, Y., Guo, J.L., Hu, Z.Q., 2013. Impact of nano zero valent iron (NZVI) on methanogenic activity and population dynamics in anaerobic digestion. Water Res. 47 (17), 6790–6800.